



**HAL**  
open science

## Optical properties of nanostructured materials: a review

François Flory, Ludovic Escoubas, Gérard Berginc

► **To cite this version:**

François Flory, Ludovic Escoubas, Gérard Berginc. Optical properties of nanostructured materials: a review . Journal of Nanophotonics, 2011, 5 (1), 10.1117/1.3609266] . hal-01790279

**HAL Id: hal-01790279**

**<https://hal.science/hal-01790279>**

Submitted on 11 May 2018

**HAL** is a multi-disciplinary open access archive for the deposit and dissemination of scientific research documents, whether they are published or not. The documents may come from teaching and research institutions in France or abroad, or from public or private research centers.

L'archive ouverte pluridisciplinaire **HAL**, est destinée au dépôt et à la diffusion de documents scientifiques de niveau recherche, publiés ou non, émanant des établissements d'enseignement et de recherche français ou étrangers, des laboratoires publics ou privés.

# Journal of Nanophotonics

[SPIDigitalLibrary.org/jnp](http://SPIDigitalLibrary.org/jnp)

## **Optical properties of nanostructured materials: a review**

François Flory  
Ludovic Escoubas  
Gérard Berginc

# Optical properties of nanostructured materials: a review

François Flory,<sup>a,b</sup> Ludovic Escoubas,<sup>b</sup> and Gérard Berginc<sup>c</sup>

<sup>a</sup>Ecole Centrale Marseille, Technopôle de château Gombert, 38 rue Joliot Curie,  
13451 Marseille cedex 13, France

[francois.flory@ec-marseille.fr](mailto:francois.flory@ec-marseille.fr)

<sup>b</sup>Aix-Marseille University, Institut Matériaux Microélectronique Nanosciences de Provence  
IM2NP CNRS UMR 6242, Campus de Saint-Jérôme, Avenue Escadrille Normandie Niemen  
Service 231, F-13397 Marseille Cedex 20, France

<sup>c</sup>Thalès Optronique S.A., 2 Avenue Gay-Lussac, 78995 Elancourt Cedex, France

**Abstract.** Depending on the size of the smallest feature, the interaction of light with structured materials can be very different. This fundamental problem is treated by different theories. If first order theories are sufficient to describe the scattering from low roughness surfaces, second order or even higher order theories must be used for high roughness surfaces. Random surface structures can then be designed to distribute the light in different propagation directions. For complex structures such as black silicon, which reflects very little light, the theory needs further development. When the material is periodically structured, we speak about photonic crystals or metamaterials. Different theoretical approaches have been developed and experimental techniques are rapidly progressing. However, some work still remains to understand the full potential of this field. When the material is structured in dimension much smaller than the wavelength, the notion of complex refractive index must be revisited. Plasmon resonance can be excited by a progressing wave on metallic nanoparticles inducing a shaping of the absorption band and of the dispersion of the extinction coefficient. This addresses the problem of the permittivity of such metallic nanoparticles. The coupling between several metallic nanoparticles induces a field enhancement in the surrounding media, which can increase phenomena like scattering, absorption, luminescence, or Raman scattering. For semiconductor nanoparticles, electron confinement also induces a modulated absorption spectra. The refractive index is then modified. The bandgap of the material is changed because of the discretization of the electron energy, which can be controlled by the nanometers size particles. Such quantum dots behave like atoms and become luminescent. The lifetime of the electron in the excited states are much larger than in continuous energy bands. Electrons in coupled quantum dots behave as they do in molecules. Many applications should be forthcoming in the near future in this field of research. © 2011 Society of Photo-Optical Instrumentation Engineers (SPIE). [DOI: [10.1117/1.3609266](https://doi.org/10.1117/1.3609266)]

**Keywords:** nanostructured thin films; surface scattering; photonic crystals; quantum dots; nanoplasmonics; solar cells.

Paper 11069V received Jun. 8, 2011; accepted for publication Jun. 14, 2011; published online 00 0, 2011.

## 1 Introduction

From atoms and molecules to crystals and bulk components, optical materials are naturally structured at different scales. Thanks to tremendous progresses in nanotechnologies, the optical materials can also be artificially structured at different scales.

The interaction of materials with optical waves and photons is strongly dependent on the structure, which can then be used to control light field distribution and light propagation. This

allows the development of a large range of key components for optical systems and it is now a major field of photonics.

Refraction, interferences, diffraction, scattering, anisotropy, absorption, light emission, and nonlinear effects are all widely used to develop photonic components. Here, we will focus our attention only on a small part of this wide field. Our purpose is to try to have a general look at linear and passive interaction of light with structured transparent materials and to give a personal view on the related phenomena. The applications are numerous and generally belong to what are called information and communication technologies in its wider meaning and green photonics, in particular photovoltaic solar cells.

The electromagnetic theory based on Maxwell equations with a rigorous approach or with more or less simplifying considerations, allows the description of light propagation in complex media when the complex refraction indices of the materials are known. We will see that the notion of refractive index must be revisited in some cases of nanometer structures. With the increase of computer power Maxwell equations can be solved, whatever the structure is, but one has to keep in mind that the sampling of spatial and temporal variables, which is necessarily finite, is still an approximation.

The general aim of photonic components is to control the way light is distributed and propagates, and its polarization and frequency.

We will consider at first surface structures. The roughness of the surface induces light scattering even with a high-quality polishing process. The surface can also be artificially structured with a periodic pattern or a random surface to have antireflecting properties or to control the light direction by diffraction. A brief review of major results in the field is discussed.

Stacking thin films of different materials and different thicknesses is the important field of optical interference coatings. Depending on deposition process and the material, the natural micro/nanostructure of the films can be more or less complex. This has different consequences on their optical properties, which are reviewed. When the films are periodically structured in one- (1D), two- (2D), or three dimensions (3D), one speaks about photonic crystals because light waves behave like the wave function of electrons in crystals. Optical interference coatings can be considered as 1D photonic crystals. Metamaterials also belongs to the photonic crystal field. The name photonic crystal is now used in a wider meaning as it can also concern nonperiodic structures.

Another field of nanophotonics that is strongly developing is the field of nanoplasmonics. It concerns the use of plasmon resonance in small metallic structures of different shapes. A lot of work is performed in this field for different applications like plasmonic circuits, plasmonic solar cells, surface enhanced Raman scattering, or tip enhanced Raman scattering. Another domain that emerged a decade ago and which is another hot topic, concerns the optical properties of quantum structures to make biological tags, efficient light emitting diodes (LEDs), efficient solar cells, or low-consumption flat panel displays. The modeling of the constitutive properties of films including quantum dots cannot be performed by the usual harmonic oscillator model. New approaches taking quantum confinement of electrons into account are discussed.

## 2 Surface Structures

### 2.1 Random Surfaces

Electromagnetic wave scattering from randomly rough surfaces and films has emerged as a discipline of considerable research in areas including surfaces optics and plasmonics. A randomly rough surface is described in terms of statistical parameters. We usually consider that there are two parts that define the surface roughness: its deviation from a plane reference surface and the variation of these heights along the surface. These surface properties are described by statistical distributions as surface height distribution functions and correlation functions that appear in the theory of wave scattering from randomly rough surfaces. In nanoscale roughness region, surfaces with large roughness height and small correlation length will have the steepest

94 slopes. Some synthetic surfaces have much larger slopes than natural surfaces. A main tool for  
95 studying these surfaces is wave scattering simulation.

96 Because of its roughness, an optical surface scatters light. In 1956, Giacomo already gave  
97 the results of measurements of the angular distribution of light scattered by Fabry-Perot filters  
98 showing scattering peaks corresponding to angle of resonances of the filter.<sup>1</sup> Since then, many  
99 works have been performed on scattering theory. For slightly rough surfaces and thin films,  
100 Kröger et al.<sup>2</sup> proposed a first order theory in 1970. The relation between the angular dependence  
101 of scattering and the statistical properties of optical surfaces was later described by Elson et al.  
102 in 1976.<sup>3</sup> Each scattering angle is related to a spatial frequency of the autocorrelation function  
103 of surface roughness. In other words, the roughness of the surface is decomposed in a sum of  
104 gratings of different steps. A spatial frequency corresponds to a step of a grating and then a  
105 scattering direction. The depth of each grating determines the scattering amplitude.

106 When concerned with multilayers made of homogeneous thin films, the roughness of each  
107 layer boundary must be taken into account. The roughness of one boundary is linked to the next  
108 with an intercorrelation function. Depending on the spatial frequency, the deposition technique,  
109 and on the material considered, this intercorrelation function can be close to one. Both a first order  
110 theory and measurement of scattering from multilayer thin films have been given by Bousquet  
111 et al. in 1981.<sup>4</sup> In this theory, a slightly rough surface is replaced by a plane surface holding a  
112 surface distribution of currents. These secondary sources send light in different directions for  
113 which the multilayer has different optical properties. The scattering diagram results from both  
114 the amplitude of these secondary sources and the transmission of the stack.

115 Different theoretical and numerical approaches have been developed to model the scattering  
116 of an electromagnetic field by random rough surfaces. The small-perturbation method<sup>5</sup> (SPM) is  
117 used for surfaces with small roughness. An overview of the method for one-dimensionally rough  
118 surfaces is given by O'Donnel in chapter 5 of Ref. 6. The Kirchhoff approximation method<sup>7</sup> is  
119 used for long correlation length surfaces, the method is described by Voronovich in Ref. 8 and  
120 in chapter 2 of Ref. 7. We can also cite the full-wave method analysis developed by Bahar,<sup>9</sup> the  
121 surface-field phase-perturbation technique developed by Ishimaru and Maradudin,<sup>10,11</sup> and the  
122 quasi-slope approximation developed by Tatarskii.<sup>12</sup> Research on numerically exact methods  
123 for randomly rough surfaces has increased over the past quarter century. Modeling rough surface  
124 scattering by exact methods often involves the choice of a one-dimension surface model due  
125 to the reduced computational complexity for these types of surfaces. But one-dimensional  
126 models are inadequate for a set of scattering effects such as cross-polarized scattering and  
127 scattering outside the plane of incidence. In the last decade, results have also been obtained by  
128 rigorous computational approaches for the scattering of polarized light from 2D randomly rough  
129 surfaces (see chapter 7 in Ref. 7 for an overview). For a randomly rough surface (i.e., stochastic  
130 problems), one can compute averages of scattered fields obtained by an ensemble of surface  
131 realizations and direct examinations of convergence are often appropriate. Problems with very  
132 large surface and Monte Carlo averaging require supercomputing resources to obtain results  
133 within a reasonable amount of time. Comparison with results obtained by analytical predictions  
134 of randomly rough surface scattering can give some insight about the accuracy of numerical  
135 computation, for example, in the case of small magnitudes of scattered intensity. We can notice  
136 that in studies of scattering from nanoscale rough surfaces, the goal is to understand the physical  
137 scattering process, subtle phenomenon whose magnitude and angle range are not very large,  
138 therefore, new analytical techniques must be developed rather than extensive use of numerical  
139 exact methods.

140 In the mid-1980s, a new popular method, called the small-slope approximation (SSA),<sup>8,13-16</sup>  
141 was proposed by Voronovich. The SSA is an appropriate candidate to bridge the gap between the  
142 Kirchhoff approximation and the small-perturbation method. It is valid for arbitrary roughness,  
143 provided that the slopes of the surface are smaller than the angles of incidence and scattering.  
144 This method has been extended up to the third-order to 3D vector cases for Gaussian and  
145 non-Gaussian randomly rough surfaces. The coherent and incoherent component formulations  
146 of the electromagnetic intensity for cross- and co-polarization have been developed in bistatic

and monostatic cases.<sup>15</sup> The SSA method has also been used to study different rough structures like a 3D slab or a film, considering the effects of higher orders in a perturbative expansion. The small slope approximation has been extended to the fourth-order terms of the perturbative development, and the expression of the cross-sections for the different polarization states can be found in Ref. 16. New formulations of the SSA are described in Ref. 16. In the development of the SSA series, the third-order SPM kernel has been taken into account. An expression of this kernel is developed in chapter 6 of Ref. 7 for 2D surfaces and a 3D slab, the development up to third order of the SPM is mandatory to analyze the phenomenon of backscattering enhancement, a well-defined peak in the retro-reflection direction of incidence for the case of nanoscale surface roughness. The Voronovich SSA was generalized to a layer bounded with two randomly rough surfaces. New terms in the SSA were introduced to consider the coupling between the two rough surfaces. Complete expressions of the scattering matrices and the expression of the needed cross-section for the different polarization states have been developed.<sup>16</sup> With this new formulation of the SSA, the backscattering enhancement for a slightly rough layer can be calculated and new analytical theories have been developed to understand the backscattering enhancement effects.<sup>17</sup>

The last problem is described by random volume and surface scattering. Useful phenomena in the optical range can be produced by random media with randomly rough surfaces. Designing these disordered slabs with rough surfaces can produce new optical components, which can transmit or scatter optical field with specified angular, spatial, or spectral properties. Understanding how light interacts with disordered matter is a fundamental issue in optoelectronics and photonics and has huge consequences in communications, imaging, and sensing. New formulations have been developed for a three-dimensional disordered medium with randomly rough interfaces.<sup>18</sup> This structure describes a device based on metallic nanoparticles embedded in insulators or dielectric media. A theory of transport based on the Bethe-Salpeter equation is presented in Ref. 18. For a three-dimensional system composed of a random medium bounded by two randomly rough surfaces, the Bethe-Salpeter equation is constructed in order that the medium and the boundaries are treated on the same footing. With this unified Bethe-Salpeter, a general expression is obtained, whatever the choice of the scattering operators used at the boundaries.

This type of simulation computation can give some experimental conditions and specifications to realize highly integrated optical devices that use metallic or metallo-dielectric nanoscale structures. For 3D slabs with nanoscale roughness and nanoparticles, the enhanced backscattering is produced by different mechanisms, the wave scattering by the same boundary, the wave coupling by the two boundaries, or the wave scattering by the random volume. All of these models and simulations can demonstrate that plasmon-polariton resonances are responsible for remarkable optical phenomena.

## 2.2 Controlled Random Surfaces

The control of surface roughness with tuned statistical properties is a mean to choose the scattered light distribution.<sup>19</sup> The method based on photofabrication using the speckle of a diffused laser beam has been proposed by Gray.<sup>20</sup> It allows tuning the statistical properties of the generated surface by modifying parameters of the exposure. Several other results based on this method have been derived after Refs. 21–23, in particular for extending depth of focus or light uniformization.<sup>24</sup> More recently, a method based on a spatial light modulator to control the laser beam shape appeared to be flexible.<sup>25</sup>

Controlling the stochastic parameters of randomly rough surfaces can be a method to “design” the scattering of an electromagnetic wave. For example, the problem is how to design a 2D randomly rough surface that scatters, in a specified manner, an optical wave incident on it and the surface realized is not a deterministic one. We notice that this kind of process is an inverse one; we must determine the structure of the surface considering the pattern of the scattered wave and the mean intensity of the scattered field, which is regarded as a spatial average of

197 the scattered intensity over an area containing many realizations of the surface roughness. A  
198 subtle question arises when we compare the definition of wave scattering from a randomly  
199 rough surface. In the case of a theoretical computation, the scattered field is averaged over  
200 the ensemble of realizations of the surface profile function. The measurement is considered on  
201 a single realization of the surface profile function. The assumption that the spatial average is  
202 equivalent to the ensemble average, can only be proven if the generated surfaces are stationary  
203 and it is not always the case. The validity of this assumption is common to all experimental  
204 work.

### 205 *2.3 Black Silicon*

206 Black silicon has been studied for more than 10 years. Black silicon texture has been produced by  
207 techniques including laser-chemical,<sup>26</sup> electrochemical,<sup>27</sup> and reactive-ion etching.<sup>28</sup> Whatever  
208 the production technique, a black silicon surface generally exhibits quasiperiodical conical  
209 structures of height and a period of a few microns (Fig. 1). In some cases, irregular nanometer Q1  
210 structures on the top of the cones make the surface more complex. Such a surface has been  
211 obtained by Mazur et al.<sup>29</sup> by sending femtosecond UV laser pulses in a SF<sub>6</sub> gas on a silicon  
212 surface. Sulphur is embedded into the silicon surface. Black silicon presents remarkable wide  
213 band antireflection properties and makes the silicon highly absorbing both in the visible and in  
214 the near infrared, below silicon band gap.<sup>30</sup>

215 Wet etching of silicon using a chloroauric acid bath is also an inexpensive way to make  
216 black silicon.

217 Reactive ion etching has also been used to replicate a photoresist pattern on a silicon Q2  
218 substrate. Troconical pyramidal shapes made by photolithography with one or two periods also  
219 gives a very wide band antireflection silicon surfaces.<sup>31,32</sup> Other techniques to make black  
220 silicon do not need photolithography. The masks are made of silica or polystyrene<sup>33-35</sup> particles  
221 directly deposited on silicon.

222 If the remarkable properties of black silicon are not yet well explained, it seems that both  
223 the structure and a possible high doping of the material may play a role. A question that is  
224 still opened concerns the smallest structures, as nanometer structures may induce quantum  
225 confinement effects.

226 A major issue arises with black silicon: can black silicon be the inexpensive way toward  
227 visible-short IR wavelength detectors? Besides HgCdTe and InGaAs, black silicon is a new way  
228 to capture visible, near infrared, and small wave infrared light.

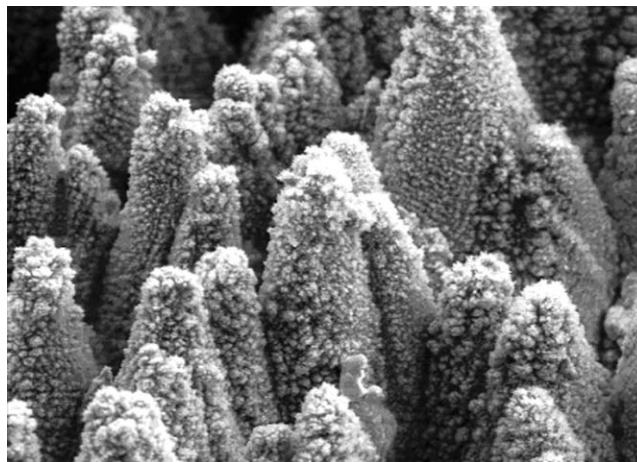


**Fig. 1** Low resolution SEM of the black silicon surface (Ref. 29).

### 3 Thin Film Structures and Optical Coatings

229

The use of interferences in multilayer coatings has been developed for many years to reduce the reflection of an optical surface, to make wavelength filters of different types like mirrors, band pass, high pass, low pass, etc. Optical coatings are now widely used in optical systems and very often they are key elements for the implementation of very important applications. Between others, low-loss mirrors are in production for gyrolasers used in automatic navigation systems. Very narrow-band pass filters are key components for dense wavelength division multiplexing optical communications or for astronomy. A very rich literature is available on this subject.<sup>36</sup>

Depending on the deposition technique used, the micro/nanostructure of thin films can be more or less complex. It is well known that low energy evaporation condensation techniques based on e-beam gun or on heated crucible give columnar thin films for most of the materials.<sup>37</sup> The typical dimension of a column is in the order of 20 nm and in some cases substructures of smaller dimension can be detected.<sup>38</sup> The refractive index is generally smaller than the refractive index of the bulk material. This is attributed to the lacunar structure of these films. In particular columnar thin films have a packing density that can be much smaller than one. The packing density is given by the ratio of the volume occupied by bulk material over the total volume of the layer.

In air, even for low moisture, water is adsorbed in the pore of the material, leading to an increase of the refractive index and then to a red shift of the optical properties of interference filters.<sup>39</sup> Under such conditions, thin film materials are made of a mixture of bulk material and vacuum or water. The problem of the refractive index of these mixed materials induced a lot of work some years ago and different models<sup>40-42</sup> taking into account the mixing have been proposed without giving a very satisfactory solution. In particular, the change induced by water adsorption cannot be fully explained. Porous films can be seen as a mixture of two materials and, following the homogenization theory, the permittivity  $\epsilon$ , i.e., the square of the refractive index, of the mixture is the weighted mean value of the  $\epsilon_1$  and  $\epsilon_2$  of the two materials. The weights are the proportions of the volume occupied by each material.

This homogenization theory was first proposed by Rytov.<sup>43</sup> In particular, he has shown that a periodic stack of films, very thin relative to the wavelength, with alternating high and low refractive indices behaves like a single-axis homogeneous material with the optical axis perpendicular to the surface.

Columnar thin films also exhibit a form birefringence. When the deposition is performed with an oblique incidence of vapor (angle  $\alpha$  in front of the normal to the surface), the columns are inclined (angle of  $\beta$ ) (Fig. 2). The relation between  $\alpha$  and  $\beta$  is approximately given by  $\tan\alpha = 2 \cdot \tan\beta$  for  $\alpha < 45^\circ$ . The anisotropy increases with an increasing angle<sup>44</sup> and the material has a biaxial behavior.<sup>45,46</sup> When the angle  $\alpha$  slowly changes during deposition, the material can have a zig-zag, an S, or a helicoidal nanostructure with a nematic or chiral behavior.<sup>47-49</sup> Such “sculptured thin films” can be classified as nanoengineered metamaterials.

The optical properties of stacks made of anisotropic layers can be calculated by the use of a  $4 \times 4$  matrix formalism.<sup>50,51</sup> Polarizing filters can be made with these materials like halfwave plates<sup>52</sup> or polarization rotator in reflection.<sup>53</sup>

With ion assisted deposition or ion beam sputtering, the deposition processes are more energetic and the materials do not exhibit columns any longer.<sup>38</sup> As they are denser, they are also insensitive to moisture.

Light can also propagate in the thickness of transparent multilayers, being trapped by total internal reflection.<sup>54</sup> The modes are then guided and the propagation constants can take only a finite number of values. A particular electric field distribution corresponds to each guided mode with the guided energy more important in one layer, several layers, or in the whole stack. A guided mode can be seen as a resonance of the optical field in the direction perpendicular to the layer boundaries. The guided mode propagation conditions correspond to constructive interferences in the direction parallel to the layer boundaries. They also correspond to poles of the reflection coefficient. The guided modes can be excited with a prism and this has been



281 widely used as characterization techniques as well for refractive index measurements<sup>55,56</sup> as for  
 282 loss measurement.<sup>54</sup> The m-line technique is now developed for gas sensing.<sup>57</sup>

## 283 **4 Photonic Crystals**

284 For optical coatings, the light is reflected or transmitted through the sample. On the contrary,  
 285 diffraction structures are generally used to distribute the light in a controlled way in different  
 286 directions of the space. The association of diffractive and interference structures in 3D compo- Q3  
 287 nents allows control, as well the directions, of propagation as the spectral distribution of the  
 288 optical waves in the space. In particular, the local field and the propagation in the structure can  
 289 be adjusted with the photon lifetime. The typical dimensions of the structure are in the order of a  
 290 part of the wavelength. These periodically structured materials are also named photonic crystals  
 291 because light waves similarly behave to the wave function of electrons in crystals.<sup>58,59</sup> Another  
 292 way to describe the light behavior in such structures is to use the density of optical modes as  
 293 Purcell defined the density of modes for electrons in solid.<sup>60</sup>

294 Photonic crystals can also be considered as metamaterials with optical properties impossible  
 295 to achieve with nonstructured materials. As an example, the structure can behave like a material  
 296 having a refractive index of zero or even negative. Many laboratories and companies pay a lot of  
 297 attention to the study of metamaterials as important applications may come soon with cloaking  
 298 properties and stealthiness or perfectly stigmatic optics. It is interesting to consider multilayer  
 299 mirrors not only as an interference system but also as a diffractive component. A mirror is a  
 300 periodic stack made of alternating high and low refractive indices, each layer having an optical  
 301 thickness of a quarter wave for the centering wavelength. It can be considered as a Bragg grating.  
 302 This concept can be extended to Bragg grating in waveguides. The main difference is that each  
 303 half period must be quarter wave but for an optical thickness defined with the effective index of  
 304 the guided mode. This principle can be used to design waveguide filters and well known optical  
 305 interference coating design methods can be helpful.<sup>61</sup>

306 As a mirror does not transmit a part of the spectrum, it has a forbidden frequency band for  
 307 photons and it is a 1D photonic crystal. Thin film Fabry-Perot filters can also be seen as photonic  
 308 bandgap structures with a defect.

## 309 **5 Optical Properties of Materials Including Quantum Structures**

310 Generally, models used to study the optical properties of nanostructures are based on the  
 311 electromagnetic theory, but when the dimension of a semiconductor nanocrystal is smaller than  
 312 the de Broglie wavelength, quantum phenomena must be considered. The de Broglie wavelength  
 313 can be seen as the coherence length of the electron wavefunction.

314 Because of their interesting electronic and luminescent properties, plenty of research con-  
 315 cerning quantum structures is performed in different laboratories.<sup>62</sup> A structure limited to a  
 316 few nm in the three dimensions of space is called quantum dot (QD). QDs have an atom-like  
 317 behavior, as the energies of the electron or hole can only take discrete sets of values. Their  
 318 absorption and luminescent spectra depend both on the properties of the semiconductor used  
 319 and on the size of the QDs. They can be very efficient light emitters with photoluminescence  
 320 quantum efficiency as high as 80%. Their emission can be continuously tuned through a large  
 321 spectrum by changing their size. As an example, CdSe QDs emit anywhere from 470 to 630 nm  
 322 by varying their size from 3 to 6.5 nm.

323 Apart from applications already implemented such as multiple quantum wells<sup>63</sup> for lasers and  
 324 detectors,<sup>64</sup> other important applications are forthcoming with the study of quantum structures.  
 325 Among others, QDs can be used to make biological tags.<sup>65</sup> More recently, they have been used  
 326 to develop high efficiency white LEDs.<sup>66</sup> They are also under study to make more efficient  
 327 OLEDs (QLED).<sup>67</sup>

328 Quantum structures are also studied to increase the photovoltaic solar cell efficiency and to  
 329 go beyond the Shockley-Queisser limit of 32% for Si based solar cells.<sup>68</sup>

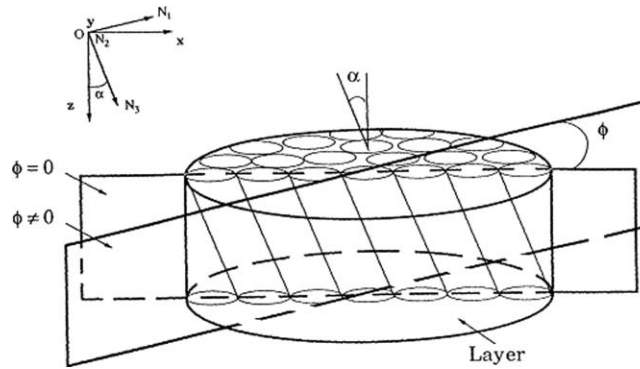


**Fig. 2** Model of anisotropy for columnar thin films.

There are two ways for enhancing the conversion efficiency. The photovoltage or the photocurrent can be increased. To increase the photovoltage, the hot carriers must be extracted from the photoconverter before they cool. The energetic hot carriers must produce two or more electron-hole pairs through impact ionization to increase the photocurrent.

In principle, QDs can be used in these two ways, which exclude one to the other in different QD solar cell configurations.<sup>69</sup> Another way to collect UV photons is to change their frequency to convert them into visible photons. QDs can also be used to make quantum dot-sensitized nanocrystalline TiO<sub>2</sub> solar cells. They can also be organized in a thin layer with an absorption band complementary to the absorption band of another material composing the solar cell.<sup>70</sup>

In most photonics components, quantum dots are embedded in thin films. So, to model the optical properties of such components, the refractive index  $n$  of thin films including quantum dots (TFIQD) must be known. The classical model used to describe  $n$  cannot apply to quantum structures and the quantization of the electron energy must be taken into account.

### 5.1 Frequency Conversion

If the radiative recombination rates of electrons generated by energetic photons are faster than cooling rates, frequency conversion can occur and can increase cell efficiency.

As an example, when considering wide band gap semiconductor nanocrystals like ZnO, the UV can be absorbed and changed into longer wavelengths. Green and UV are emitted. The luminescence in the green is not completely explained but it can be due to oxygen vacancies.<sup>71</sup> The luminescence in the UV is coming from quantum confinement with an energy level close to the edge of the bandgap. The UV shift of the bandgap is well explained by calculation (Fig. 3).<sup>72</sup>

In this case of luminescence, the charges generated by the UV photons must radiatively relax before being transferred to the surrounding media, being recombined at the nanocrystal surfaces, or being coupled to phonon nonradiative decays.

### 5.2 Charge Carrier Generation

Depending of their size, CdSe nanoparticles produce electrons and holes from different photon energies of the visible spectrum. The charges can be transferred to the surrounding medium if resonant transfers are possible. These particles can replace dye molecules in TiO<sub>2</sub> sensitized dye.<sup>73</sup> It is interesting to notice that, thanks to the relative band offset, CdSe quantum dots have a resonant electron energy level with the conduction band of TiO<sub>2</sub>. “Rainbow” solar cells using CdSe of different-sized quantum dots assembled in an orderly fashion are under study.<sup>74</sup>

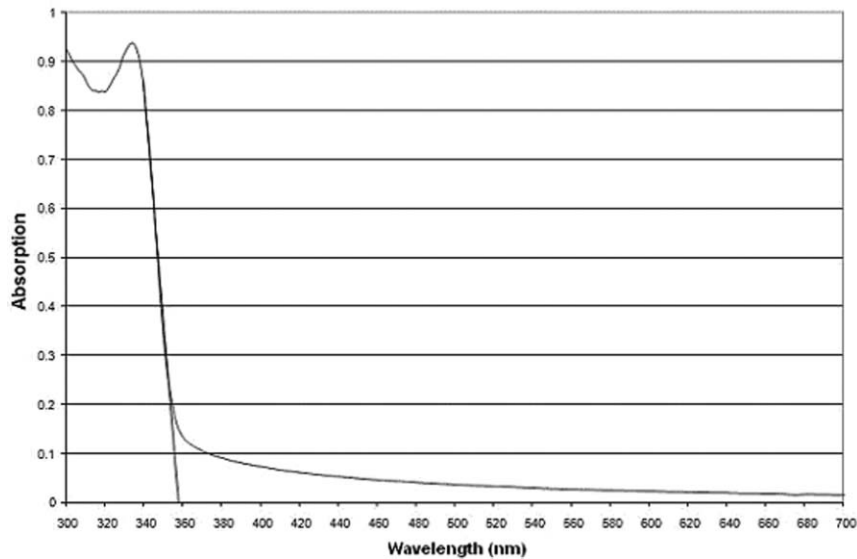


**Fig. 3** Absorption spectrum of ZnO nanocrystals in a solution of MeOH.

362 Hybrid organic/inorganic cells can also be made with P3HT and CdSe nanorods or P3HT  
 363 and PbS nanoparticles. With size-quantized PbS nanoparticles, 3% incident photon to current  
 364 efficiencies (IPCE) under 550-nm monochromatic irradiation is obtained.<sup>75</sup> A 6.9% IPCE under  
 365 0.1 milliwatt per square illumination at 515 nm is obtained with 7-nanometer by 60-nanometer  
 366 CdSe nanorods.<sup>76</sup>

### 367 *5.3 Multiple Exciton Generation*

368 When photoexcited carriers elastically collide with one another, no energy is lost. On the  
 369 contrary, collisions with the atoms of the cell material are inelastic. They induce an energy loss  
 370 with phonon induced decays. In principle, if atomic collisions can be avoided during the time  
 371 it takes a photogenerated carrier to cross the cell, such a thermalization loss can be avoided.  
 372 Carriers either have to go through the cell very quickly or cooling rates have to be slowed in  
 373 some way. If, instead of giving up their excess energy as heat, the high energy electron-hole  
 374 pairs are used to create additional pairs, higher efficiency would be possible (Fig. 4). This can  
 375 be achieved by using QDs because of the longer lifetime of the discrete excited states. The  
 376 creation of more than one pair by high energy photons has attributed to impact ionization by  
 377 the photoexcited carriers. In such a case, many electron-hole pairs could be generated by each  
 378 incident photon (Fig. 5).<sup>77</sup>

379 In principle, MEG can give up to 75% efficient conversion. To the best of our knowledge,  
 380 only the Auger principle has been demonstrated, but there may be different competing processes.  
 381 Charge cooling because of phonon coupling is, of course, one of them but also, if the absorption  
 382 occurs into the wrong state, there will be no impact ionization. Auger recombination after decay  
 383 can also happen.

### 384 *5.4 Optical Properties of Thin Films Including Quantum Dots*

385 The value of the complex refractive index or permittivity is needed to calculate the optical  
 386 properties of photonic structures. The bulk value of the refractive index is not fitted when the  
 387 materials are structured in small dimensions and the classical model<sup>78-80</sup> cannot be used.

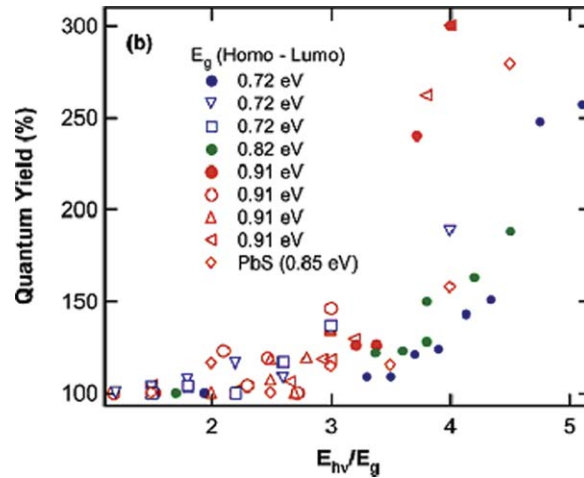


**Fig. 4** Quantum yield versus the relative energy of photons in front of the material bandgap showing multiple exciton generation with PbSe nanoparticles.

A model for quantum wells can be used as a first theoretical model. Many works have already been performed on single and periodic quantum wells of square and nonsquare profiles.<sup>81,82</sup> The model presented in Ref. 72 based on the approximation of the effective mass, can be applied to single wells, coupled periodic, and nonperiodic multiple wells and to stacks of wells of any depth and any width. The main advantages of this model are its easy implementation and its small computation time.

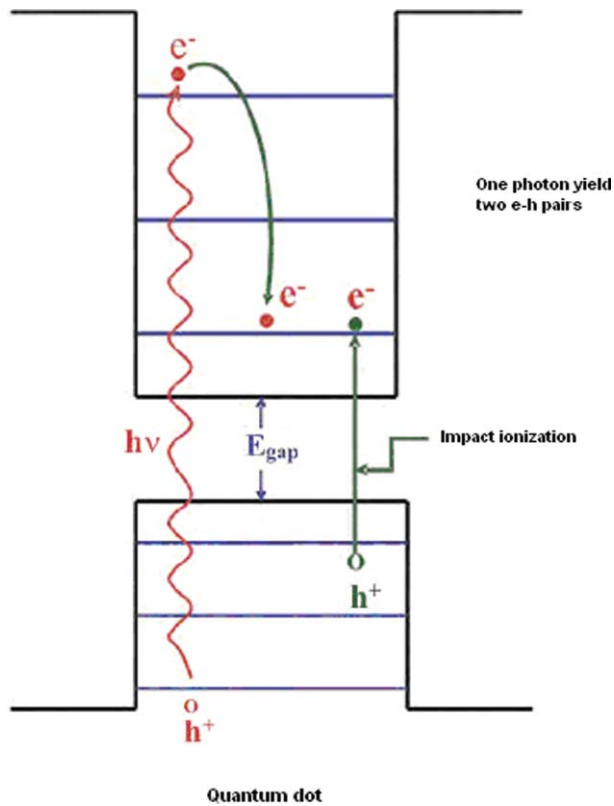


**Fig. 5** Sketch of a multiple exciton generation process.

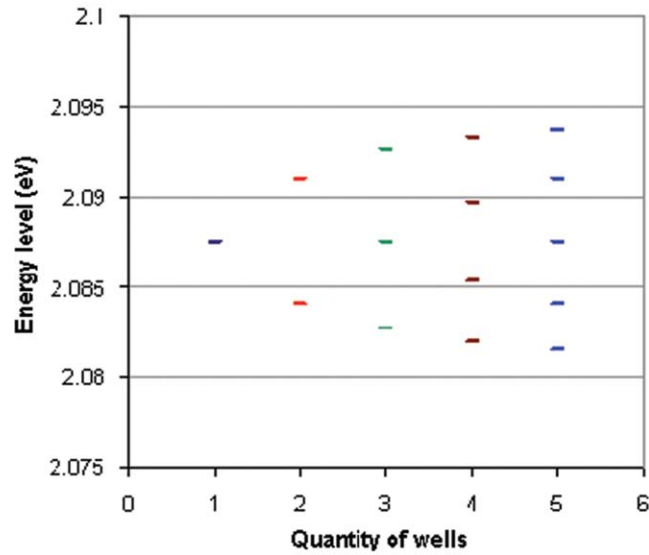


**Fig. 6** Splitting of the highest energy level of electrons in coupled quantum wells, when considering from left to right 1, 2, 3, 4, and 5 identical coupled wells. Each well has a depth of 2.9 eV, a width of 1 nm and the distance between the wells is also 1 nm.

394 In a multiple well, a recurrent relation can be found for the function  $Q = \frac{1}{m} \frac{d\psi}{dx} / \psi$ , where  $\psi$   
 395 is the electron wave function and  $x$  is the direction perpendicular to the well boundaries

$$Q_j = k_j \frac{Q_{j-1} - k_j \tan(k_j a_j)}{Q_{j-1} \tan(k_j a_j) + k_j}, \quad (1)$$

396 with  $j$  referring to a well boundary in the structure. The width of the  $j$ th layer is  $a_j$  and  $k_j = \chi_j$   
 397 for  $E > V_j$  or  $-i\gamma_j$  for  $E < V_j$ . The function  $Q$  is continuous, crossing a potential barrier. So,  
 398 the value of  $Q$  on one limit of a structure can be obtained as a function of  $Q$  on its other limit.

399 If the electron is confined in the structure,  $\psi$  is evanescent in the surrounding media. The  
 400 equation describing the possible discrete energy levels is then derived from these considerations.

401 The wavefunction and the square of its modulus giving the electron density probability  
 402 distribution, can then be calculated in the whole structure

$$\Psi_j(x) = C_j^+ \left[ e^{ik_j x} + \frac{ik_j - Q_{j-1}}{Q_{j-1} + ik_j} e^{ik_j(2x_{j-1} - x)} \right], \quad (2)$$

403 where  $C_j^+$  is a constant that can be normalized.  $k_j = \chi_j$  for  $E > V_j$  or  $-i\gamma_j$  for  $E < V_j$   
 404 with  $\chi_j^2 = 2m/\hbar^2(E - V_j)$  and  $\rho_j^2 = 2m/\hbar^2(V_j - E)$ . For each possible value of the energy  
 405  $\int |\psi|^2 dx = 1$ .

406 In identical coupled wells, the energy levels of the single well are split (Figs. 6 and 7) and  
 407 when there are a large number of coupled wells, they become energy bands. In nonperiodic  
 408 structures, the electrons can be localized or delocalized like electrons in molecules (Fig. 8). It  
 409 is worth noticing that the properties of the charges can then be engineered, to some extent, by  
 410 adapting the size of the QDs and their coupling distance.

411 A lot of new applications are expected to come with such artificial molecules.

412 As for electrons, the energy levels of the holes can be calculated in quantum wells. The  
 413 optical properties of quantum wells can then be deduced from the electron and hole energy  
 414 distribution. An example of a model is proposed in Ref. 83 for the complex refractive index  
 415 dispersion with a wavelength of interdiffused quantum wells. In the case of a film composed  
 416 of quantum dot semiconductor embedded in a homogeneous matrix, the refractive index can be

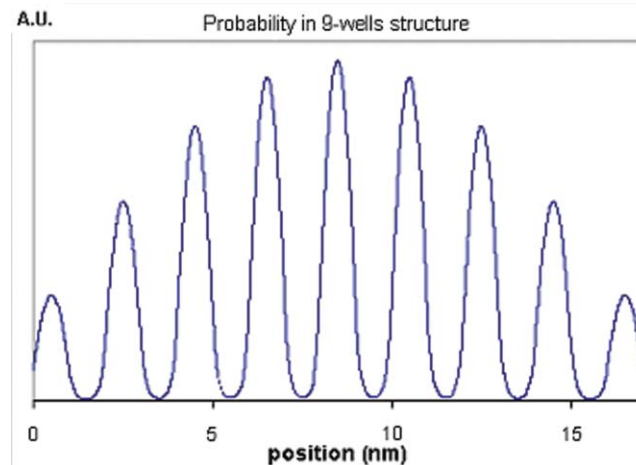


**Fig. 7** Electron density of probability for the lowest energy level in a structure composed of nine identical coupled wells.

calculated from the refractive index of the quantum dots and the refractive index of the matrix 417  
by using the homogenization theory. 418

Knowing the energy levels of electrons and holes in a quantum structure<sup>84</sup> and taking into 419  
account the band broadening phenomena induced by size dispersion and coupling effects, the 420  
absorption dispersion with wavelength can be approximately calculated. But the amplitude 421  
of the absorption in QDs cannot be directly calculated as it depends on their absorption cross 422  
section, which has not yet been modeled. The absorption amplitude can then be only obtained by 423  
measurement. By measuring  $R(\lambda)$  and  $T(\lambda)$  of a thin film including quantum dots, the extinction 424  
coefficient dispersion is deduced from the absorption  $A(\lambda) = 1 - R(\lambda) - T(\lambda)$  425

$$k(\lambda) = -\frac{\lambda}{4\pi d} \text{Log}(A(\lambda)), \quad (3)$$

Q4 with  $d$  the thickness of the film. By using Kramers-Krönig relations, the dispersion of the real 426  
part of the refractive index of the TFIQD can be obtained. As to have quantum confinement, 427

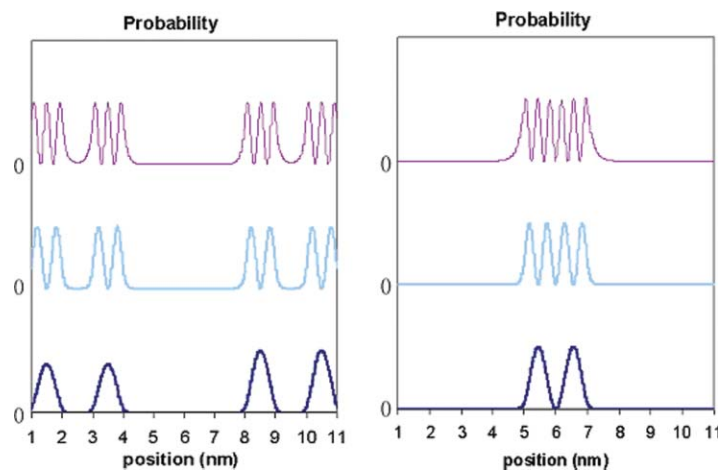


**Fig. 8** Electron density of probability in a nonperiodic structure composed of five coupled wells of depth 2.9 eV, of widths 1, 1, 2, 1, and 1 nm, respectively. The distance between each well is 1 nm.

428 the bandgap of the QDs must be smaller than that of the surrounding material, the absorption  
 429 is mainly due to the QDs for the wavelengths just shorter than the QDs bandgap. In this  
 430 spectral region, the measured absorption dispersion with wavelength should correspond to the  
 431 calculation.

432 So, research on quantum structures for photovoltaic cells is very active. In the near future,  
 433 many progresses are expected to develop high-efficient and low-cost solar cells. The control of  
 434 the material structures at a nanometer level is mandatory to fully benefit from the attractive Q5  
 435 properties of QDs of different sizes and made of different materials. Coupled QDs could also  
 436 lead to new useful structures for many different applications.

## 437 6 Nanoplasmonics

438 The free electrons at a planar surface between a metal and a dielectric material can exhibit  
 439 a collective oscillation of free electrons at a resonant frequency. The corresponding surface-  
 440 plasmon-polariton (SPP) electromagnetic wave of TM polarization propagates along the surface.  
 441 This surface wave can only be excited with an evanescent wave. A totally reflecting prism can  
 442 be used for that purpose.<sup>85</sup>

443 When considering metallic nanoparticles of dimension of a few tens of nanometer, the SSP  
 444 can be excited on the nanoparticle surfaces.<sup>86</sup> The two key interest areas are 1. the ability  
 445 to channel light into sub-wavelength zones and 2. the local optical electric field is strongly  
 446 enhanced on the metal surface thanks to plasmon resonance. This can be used to increase the  
 447 absorption in the surrounding material or to enhance fluorescence and Raman scattering.

448 As the propagation length of a SPP is generally longer than the circumference of the metallic  
 449 nanoparticle, the electric field amplitude is modulated on the surface. If several nanoparticles are  
 450 close enough to be coupled, the optical electric field is also increased in the medium between the  
 451 nanoparticles. The resonance and its width depend, of course, on the metal used but also on the  
 452 size, the shape of the nanoparticle, and the dielectric properties of the surrounding medium. It can  
 453 take place in the visible or in the infrared. The SPPs has a TM polarization when the dielectric Q6  
 454 media is isotropic but multiple modes of SPP-wave propagation with different polarization states  
 455 can be simultaneously supported by a metal/structured thin film interface.<sup>87</sup>

456 The plasmonics features have been extensively studied by the international scientific com-  
 457 munity and are considered as extremely promising.<sup>88</sup> Optical nanoantennas based on metallic  
 458 nanostructures will boost the efficiency of light-matter interactions.<sup>89</sup> This electromagnetic  
 459 enhancement plays a key role in surface enhanced techniques: surface enhanced Raman spec-  
 460 troscopy, surface enhanced fluorescence, surface enhanced infrared absorption, etc. Using Q7  
 461 these techniques, single molecule detection can now be achieved.<sup>90</sup> The correlation between the  
 462 observed electromagnetic enhancement and the plasmonic properties of these nanoantennas is  
 463 heavily studied.

464 Highly efficient plasmonic nanostructures are also required for further development of new  
 465 optical near-field techniques such as tip enhanced Raman spectroscopy.<sup>91</sup> Q8

466 Nanoplasmonic is also under study to make plasmonic optical circuits,<sup>92</sup> highly efficient  
 467 light emitting diodes,<sup>93</sup> and extremely sensitive chemical and biochemical sensors.<sup>94</sup>

468 Plasmonics has a great interest in the photovoltaic domain in order to improve the photonic  
 469 absorption, thus, the solar cell efficiency.<sup>95</sup> For this application, the aim of plasmonics is to excite  
 470 localized plasmons by using metallic nanoparticles to trap or confine light inside the photoactive  
 471 material, or to obtain beneficial resonant internal light scattering on these metallic particles.<sup>96-98</sup>  
 472 This excitation depends on several parameters such as the metal nature, the surface density of the  
 473 particles, their diameter, the incident angle of light, the wavelength, the polarization, etc. Light  
 474 absorption in the active material can then be increased, in particular in the spectral ranges where  
 475 the photovoltaic material only weakly absorbs the light. As an example, one of the best power  
 476 efficiencies for an organic solar cell [6.5%, Ref. 99] is based on an active donor:acceptor bulk  
 477 heterojunction, the P3HT:PCBM. Its low cutting wavelength (close to 650 nm, i.e., a bandgap  
 478 around 2.1 eV) greatly limits the efficiency. Enhancing light absorption around this spectral

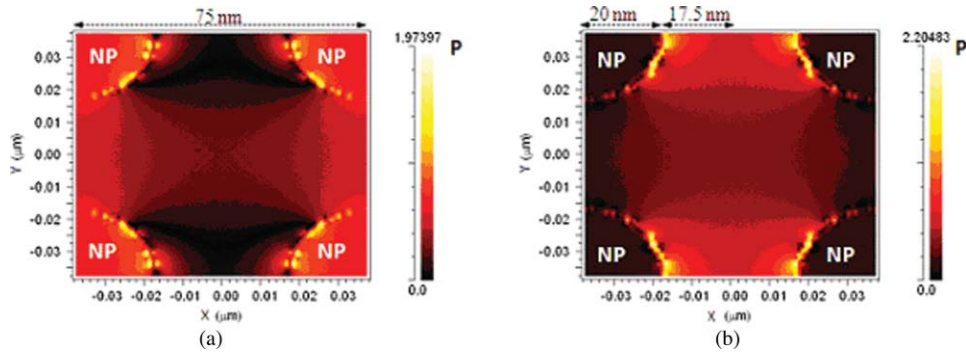


**Fig. 9** Electromagnetic power density distribution in the plane  $\{x, y\}$  for an array of four silver nanoparticles (NPs) embedded in a dielectric material. Incident wavelength: (a) 450 and (b) 600 nm.

range where solar intensity is maximum is the current challenge. As a consequence, a precise and highly efficient characterization of optical nanoantennas used in such devices is essential and can be seen as a real challenge. Unfortunately, it remains a “largely unexplored terrain.”<sup>88</sup>

Today, many theoretical calculations [finite-difference time-domain (FDTD), for instance] have clearly demonstrated the nature and the spatial localization of the electromagnetic field in the vicinity of metallic nanoparticles. As an example, the electric field distribution calculated with the FDTD method in a poly [2-méthoxy-5-(2-éthyl-hexyloxy)-1, 4-phénylène-vinylène]: 6, 6-phenyl C61-butyric acid methyl ester (MEH-PPV:PCBM) bulk heterojunction including silver nanospheres is shown in Fig. 9. A comparison between the absorption with and without nanoparticles of such a heterojunction is given in Fig. 10.<sup>100,101</sup>

Nevertheless, it remains extremely difficult to have an experimental nanometer localization of the enhanced electromagnetic field. In classical surface enhanced spectroscopy, the final optical signal is measured in far field and the precise localization of hot spots remains impossible due to the poor resolution. As a consequence, it appears extremely difficult to validate the nature of the enhanced electromagnetic field obtained with theoretical calculations by experimental

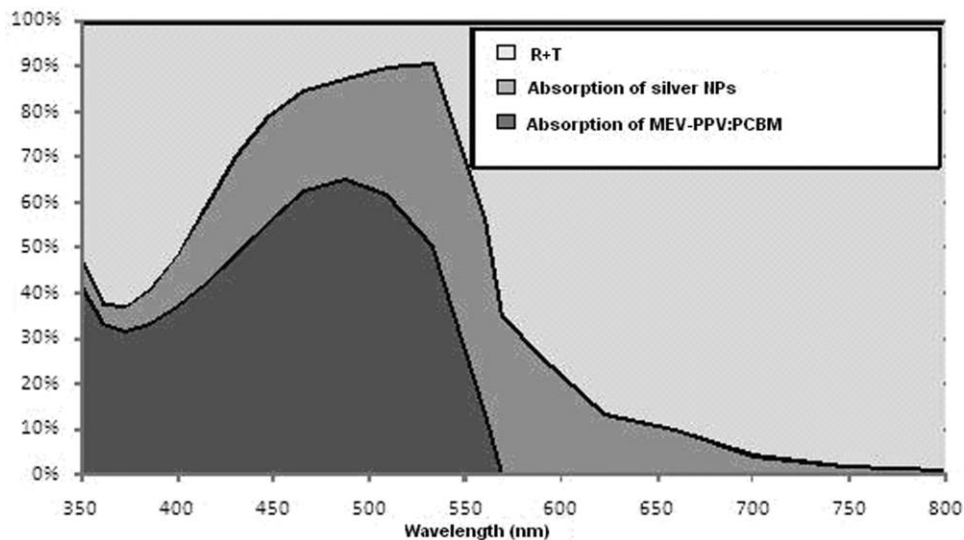


**Fig. 10** Intrinsic absorption of MEH-PPV:PCBM (light gray), silver NPs (black), and absorption losses (reflection and transmission) (dark gray) for a structure with NP diameters of 100 nm and period of 200 nm.



494 measurements. Some experimental works have already been performed, but this remains an  
495 important topic of study.

## 496 7 Conclusions

497 With an increasing capability of structuring materials at a smaller and smaller scale, one can  
498 access more and more precise control of light/material interaction. We can expect to organize  
499 the propagation of optical waves as well, close to the material in the near field as at any distance  
500 of it.

501 Random surface structures that control statistical properties are developed to shape, at will,  
502 the bidirectional reflectance distribution function (BRDF) of surface. Wide-band antireflection Q9  
503 structures are rapidly progressing but also deeply etched surfaces like black silicon appear to  
504 exhibit remarkably strong absorption and antireflection properties even in the infrared. The  
505 inhomogeneities and the structure of thin films can now be partly controlled. This is used to  
506 make materials with defined refractive index with, in particular, birefringent properties of high  
507 interest for applications.

508 Photonic crystals have also experienced a very strong development these last years in  
509 particular with the metamaterials. New developments are now taking place with nanomagnetic Q10  
510 structures. But when the structure can be controlled at a smaller size of a few thousands atoms,  
511 a new field is opening with a control of intimate properties of matter.

512 Quantum confinement, which can be used to tune the properties of electrons, must lead to  
513 completely new applications where electrons and photons must be considered together. The  
514 concept of permittivity is then revisited.

515 This concept is also different for metallic nanoparticles embedded in a dielectric material and  
516 the association of plasmon resonance and scattering again concerns both electron and photons.

517 Though not discussed in this paper, the dynamic properties of electrons and the nonlinear  
518 optical properties have yet to be jointly considered and a lot of research has yet to be performed  
519 in these fields. This should pave the way to more and more complex applications at low cost,  
520 well suited to nomadism, for every day life, energy, security, environment, and health.

## 521 References

- 522 1. P. Giacomo, "Les couches réfléchissantes multidiélectriques appliquées à l'interférométrie  
523 de Fabry-Perot. Étude théorique et expérimentale des couches réelles," *Rev. Opt., Theor.*  
524 *Instrum.* **35**, 317–354 (1956). Q11
- 525 2. E. Kröger and E. Kretschmann, "Scattering of light by slightly rough surfaces on thin  
526 films including plasma resonance emission," *Z. Phys.* **237**, 1–15 (1970).
- 527 3. J. M. Elson and J. M. Bennett, "Relation between the angular dependence of scattering  
528 and the statistical properties of optical surfaces," *J. Opt. Soc. Am.* **69**, 31–47 (1979).
- 529 4. P. Bousquet, F. Flory, and P. Roche, "Scattering from multilayer thin films: Theory and  
530 experiment," *J. Opt. Soc. Am.* **71**(9), 1115–1123 (1981).
- 531 5. S. O. Rice, "Reflection of electromagnetic waves from slightly rough surfaces," *Commun.*  
532 *Pure Appl. Math.* **4**, 351–378 (1951).
- 533 6. A. A. Maradudin, *Light Scattering and Nanoscale Surface Roughness*, Springer, New  
534 York (2007).
- 535 7. A. Beckmann and A. Spizzichino, *The Scattering of Electromagnetic Waves from Rough*  
536 *Surfaces*, Pergamon press, New York (1963). Q12
- 537 8. A. G. Voronovich, *Wave Scattering from Rough Surfaces*, Springer-Verlag, Berlin (1994).
- 538 9. E. Bahar, "Full wave solutions for the depolarization of the scattered radiation fields by  
539 rough surfaces of arbitrary slopes," *IEEE Trans. Antennas Propag.* **29**, 443–454 (1981).
- 540 10. J. Shen and A. A. Maradudin, "Multiple scattering of waves from random rough surfaces,"  
541 *Phys. Rev. B* **22**, 4234–4240 (1980). Q13

11. D. P. Winebrenner and A. Ishimaru, "Investigation of a surface field phase-perturbation technique for scattering from rough surfaces," *Radio Sci.* **20**, 161–170 (1985). 542
12. V. I. Tatarskii, "The expansion of the solution of the rough surface scattering problem in powers of quasi-slopes," *Waves Random Media* **3**, 127–146 (1993). 543
13. A. G. Voronovich, "Small-slope approximation in wave scattering by rough surfaces," *Sov. Phys. JETP* **62**, 65–70 (1985). 544
- Q14 14. A. G. Voronovich, "Small-slope approximation for electromagnetic wave scattering at a rough interface of two dielectric halfspace," *Waves Random Media* **4**, 337–367 (1994). 545
15. G. Berginc, "Small-slope approximation method: A further study of vector wave scattering from two-dimensional surfaces and comparison with experimental data," *Prog. Electromagnetics Res., PIER* **37**, 251–287 (2002). 546
16. G. Berginc and C. Bourrely, "The small slope approximation method applied to a three dimensional slab with rough boundaries," *PIER* **73**, 131–211 (2007). 547
17. C. Bourlier and G. Berginc, "Multiple scattering in the high-frequency limit with second-order shadowing function from 2-D anisotropic rough dielectric surfaces: I Theoretical study," *Waves in Random Media* **14**, 229–252 (2004); **14**, 253–276 (2004). 548
- Q15 18. G. Berginc and C. Bourrely, "Light scattering from 3D nanoscale disordered media," *PIERS Online* **6**(8), 730–734 (2010). 549
19. A. A. Maradudin, Ed., *Structured Surfaces as Optical Metamaterials*, Cambridge University, Cambridge, England (2011). 550
20. P. F. Gray, "Method of forming optical diffusers of simple known statistical properties," *Opt. Acta* **25**(8), 765–775 (1978). 551
21. E. R. Mendez, M. A. Ponce, V. Ruizcortes, and Z. H. Gu, "Photofabrication of one-dimensional rough surfaces for light-scattering experiments," *Appl. Opt.* **30**(28), 4103–4112 (1991). 552
22. E. R. Mendez, E. E. Garcia-Guerrero, H. M. Escamilla, A. A. Maradudin, T. A. Leskova, and A. V. Shchegrov, "Photofabrication of random achromatic optical diffusers for uniform illumination," *Appl. Opt.* **40**, 1098–1108 (2001). 553
23. E. R. Mendez, T. A. Leskova, A. A. Maradudin, M. Leyva-Lucero, and J. Munoz-Lopez, "The design of two-dimensional random surfaces with specified scattering properties," *J. Opt. A, Pure Appl. Opt.* **7**, 141–151 (2005). 554
24. E. E. Garcia-Guerrero, E. R. Mendez, and H. M. Escamilla, "Design and fabrication of random phase diffusers for extending the depth of focus," *Opt. Express* **15**, 910–923 (2007). 555
25. V. Brissonneau, L. Escoubas, F. Flory, G. Berginc, G. Soriano, G. Maire, and H. Giovannini, "Laser assisted fabrication of random rough surfaces for optoelectronics," to be published in *Appl. Surf. Sci.* (2011). 556
- Q16 26. T.-H. Her, R. J. Finlay, C. Wu, S. Deliwala, and E. Mazur, "Microstructuring of silicon with femtosecond laser pulses," *Appl. Phys. Lett.* **73**, 1673–1675 (1998). 557
27. L. L. Ma, Y. C. Zhou, N. Jiang, X. Lu, J. Shao, W. Lu, J. Ge, X. M. Ding, and X. Y. Hou, "Wide-band 'black silicon' based on porous silicon," *Appl. Phys. Lett.* **88**, 171907 (2006). 558
28. T. P. Chow, P. A. Maciel, and G. M. Fanelli, "Reactive Ion Etching of Silicon in CCl<sub>4</sub> and HCl Plasmas," *J. Electrochem. Soc.* **134**, 1281–1286 (1987). 559
- Q17 29. T. H. Her, R. J. Finlay, C. Wu, and E. Mazur, "Femtosecond laser-induced formation of spikes on silicon," *Appl. Phys. A: Mater. Sci. Process.* **70**(4), 383–385 (2000). 560
30. C. Wu, C. H. Crouch, L. Zhao, J. E. Carey, R. Younkin, J. A. Levinson, E. Mazur, R. M. Farrell, P. Gothoskar, and A. Karger, "Near-unity below-band gap absorption by microstructured silicon," *Appl. Phys. Lett.* **78**, 1850–1852 (2001). 561
31. R. Bouffaron, L. Escoubas, J. J. Simon, P. Torchio, F. Flory, G. Berginc, and P. Masclet, "Enhanced antireflecting properties of micro-structured top-flat pyramids," *Opt. Express* **16**(23), 19304–19309 (2008). 562

- 595 32. L. Escoubas, R. Bouffaron, V. Brissonneau, J. J. Simon, G. Berginc, F. Flory, and  
 596 P. Torchio, “Sand-castle bi-periodic pattern for spectral and angular broadening of an-  
 597 tireflective properties,” *Opt. Lett.* **35**(9), 1455–1457 (2010).
- 598 33. C. H. Sun, P. Jiang, and B. Jiang, “Broadband moth-eye antireflection coatings on silicon,”  
 599 *Appl. Phys. Lett.* **92**, 061112 (2008).
- 600 34. Y. J. Zhang, W. Li, and K. J. Chen, “Application of two-dimensional polystyrene ar-  
 601 rays in the fabrication of ordered silicon pillars,” *J. Alloys Compd.* **450**(1–2), 512–516  
 602 (2008).
- 603 35. Y. J. Zhang, X. H. Wang, Y. X. Wang, H. L. Liu, and J. H. Yang, “Ordered nanos-  
 604 tructures array fabricated by nanosphere lithography,” *J. Alloys Compd.* **452**(2), 473–477  
 605 (2008).
- 606 36. H. A. Macleod, *Thin-Film Optical Filters*, 4th ed., Chemical Rubber, Boca Raton (2010).
- 607 37. G. Dirks and H. J. Leamy, “Columnar microstructure of optical thin films,” *Thin Solid*  
 608 *Films* **47**, 219–222 (1997).
- 609 38. F. Flory and L. Escoubas, “Optical properties of nanostructured thin films,” *Prog. Quantum*  
 610 *Electron.* **28**, 89–112 (2004).
- 611 39. S. Ogura and H. A. Macleod, “Water sorption phenomena in optical thin films,” *Thin Solid*  
 612 *Films* **34**, 371–375 (1976).
- 613 40. K. Kinoshita and M. Nishibori, “Effects of vacuum exposure on stress and spectral shift of  
 614 high reflective coatings,” *J. Vac. Sci. Technol.* **6**, 730–733 (1969).
- 615 41. J. C. Maxwell-Garnett, “Colors in metal glasses and in metal films,” *Philos. Trans. R. Soc.*  
 616 **203**, 385–419 (1904). Q18
- 617 42. W. L. Bragg and A. B. Pippard, “The form birefringence of macromolecules,” *Acta*  
 618 *Crystallogr.* **6**, 865–867 (1953).
- 619 43. S. Rytov, “Electromagnetic properties of a finely stratified medium,” *Sov. Phys. JETP* **2**,  
 620 466–474 (1956).
- 621 44. H. Jänchen, D. Endeleva, N. Kaiser, and F. Flory, “Determination of the refractive indices  
 622 of highly biaxial anisotropic coatings using guided modes,” *Pure Appl. Opt.* **5**(4), 405–415  
 623 (1996).
- 624 45. F. Flory, D. Endeleva, E. Pelletier, and I. Hodgkinson, “Anisotropy in thin films. Mod-  
 625 elization and measurement of guided and non guided optical properties. Application to  
 626 TiO<sub>2</sub> films,” *Appl. Opt.* **32**(28), 5649–5659 (1993).
- 627 46. F. Horowitz and H. A. Macleod, “Form birefringence in thin films,” *Proc. SPIE* **380**,  
 628 83–87 (1983).
- 629 47. K. Robbie, M. J. Brett, and A. Lakhtakia, “Chiral sculptured thin films,” *Nature* **384**, 616  
 630 (1996). Q19
- 631 48. A. Lakhtakia and R. Messier, “Sculptured thin films,” *Nanometer Structures: The-*  
 632 *ory, Modeling, and Simulation*, A. Lakhtakia, Ed., SPIE Press, Washington, WA  
 633 (2004). Q20
- 634 49. A. Lakhtakia and R. Messier, *Sculptured Thin Films: Nanoengineered Morphology and*  
 635 *Optics*, SPIE Press, Washington, WA (2005).
- 636 50. D. Berreman, “Optics in stratified and anisotropic media: 4×4 matrix formulation,” *J. Opt.*  
 637 *Soc. Am.* **62**, 502–510 (1972).
- 638 51. I. Hodgkinson and H. Wu, *Birefringent Thin Films and Polarizing Elements*, World Sci-  
 639 entific, Singapore (1997).
- 640 52. T. Motohiro and Y. Taga, “Thin film retardation plate by oblique deposition,” *Appl. Opt.*  
 641 **28**, 2466–2482 (1989).
- 642 53. F. Flory, L. Escoubas, and B. Lazaridés, “Artificial anisotropy and polarizing filters,”  
 643 *Appl. Opt.* **41**(16), 3332–3335 (2002).
- 644 54. F. Flory, “Characterization: Guided wave techniques,” *Thin Films for Optical Systems*, F.  
 645 Flory, ed., Marcel Dekker, New York (1995).

55. S. Monneret, P. Huguet-Chantôme, and F. Flory, “m-Lines technique: Prism coupling measurement and discussion of accuracy for homogeneous waveguides,” *J. Opt. A, Pure Appl. Opt.* **2**(3), 188–195 (2000). 646
56. J. Massaneda, F. Flory, and E. Pelletier, “Determination of the refractive index of layers in a multilayer stack by guided wave technique,” *Appl. Opt.* **38**, 19, 4177–4181 (1999). 647
- Q21 57. T. Mazingue, L. Escoubas, L. Spalluto, F. Flory, G. Socol, C. Ristoscu, E. Axente, S. Grigorescu, I. N. Mihailescu, and N. A. Vainos, “Nanostructured ZnO coatings grown by pulsed laser deposition for optical gas sensing of butane,” *J. Appl. Phys.* **98**, 074312 (2005). 648
58. D. Kossel, “Analogies between thin-film optics and electron band theory of solids,” *J. Opt. Soc. Am.* **568**, 1434 (1966). 649
- Q22 59. K. Sakoda, *Optical Properties of Photonic Crystals*, 2nd ed., Springer-Verlag, Berlin (2004). 650
60. E. M. Purcell, “Spontaneous emission probabilities at radio frequencies,” *Phys. Rev.* **69**, 681 (1946). 651
- Q23 61. L. Escoubas, E. Drouard, and F. Flory, “Designing waveguide filters with optical thin-film computational tools,” *Opt. Commun.* **197**, 309–316 (2001). 652
62. A. Lakhtakia, Ed., *Nanometer Structures: Theory, Modeling, and Simulation*, SPIE Press, Washington (2004). 653
- Q24 63. P. S. Zory, “The origin of quantum wells and the quantum well laser,” in *Quantum Well Lasers*, C. H. Henry Jr., Ed., Academic, New York (1993), pp. 1–13. 654
64. H. Schneider and H. Liu, *Quantum Well Infrared Photodetectors: Physics and Applications*, Springer-Verlag, Berlin (2006). 655
65. M. Bruchez, M. Moronne, P. Gin, S. Weiss, and A. P. Alivistos, “Semiconductor nanocrystals as fluorescent biological labels,” *Science* **281**, 1201–1205 (1998). 656
- Q25 66. S. Nizamoglu, G. Zengin, and H. V. Demir, “Color-converting combinations of nanocrystal emitters for warm-white light generation with high color rendering index,” *Appl. Phys. Lett.* **92**, 031102 (2008). 657
67. S. Coe, W. K. Woo, M. Bawendi, and V. Bulovic, “Electroluminescence from single monolayers of nanocrystals in molecular organic devices,” *Nature* **420**, 800–803 (2002). 658
68. W. Shockley and H. J. Queisser, “Detailed balance limit of efficiency of *p/n* junction solar cells,” *J. Appl. Phys.* **32**, 510–519 (1961). 659
69. P. V. Kamat, “Quantum dot solar cells. Semiconductor nanocrystals as light harvesters,” *J. Phys. Chem. C* **112**, 18737–18753 (2008). 660
70. O. V. Vassiltsova, S. K. Panda, Z. Zhao, M. A. Carpenter, and M. A. Petrukhina, “Ordered fabrication of luminescent multilayered thin films of CdSe quantum dots,” *Dalton Trans.* 9426–9432 (2009). 661
71. S. A. Studenikin, N. Golego, and M. Cocivera, “Fabrication of green and orange photoluminescent, undoped ZnO films using spray pyrolysis,” *J. Appl. Phys.* **84**(4), 2287–2294 (1998). 662
72. F. Flory, Y.-J. Chen, C.-C. Lee, L. Escoubas, J.-J. Simon, P. Torchio, J. Le Rouzo, S. Vedraïne, H. Derbal-Habak, I. Shupyk, Y. Didane, and J. Ackermann, “Optical properties of dielectric thin films including quantum dots,” *Appl. Opt.* **50**(9), C129–C134 (2011). 663
73. I. Robel, V. Subramanian, M. Kuno, and P. V. Kamat, “Quantum dot solar cells. Harvesting light energy with CdSe nanocrystals molecularly linked to mesoscopic TiO<sub>2</sub> films,” *J. Am. Chem. Soc.* **128**, 2385–2393 (2006). 664
74. A. Kongkanand, K. Tvrdy, K. Takechi, M. Kuno, and P. V. Kamat, “Quantum dot solar cells. Tuning photoresponse through size and shape control of CdSe-TiO<sub>2</sub> architecture,” *J. Am. Chem. Soc.* **130**, 4007–4015 (2008). 665
75. S. Günesa, H. Fritz, N. S. Neugebauer, S. Sariciftcia, Kumar, and G. D. Scholes, “Hybrid solar cells using PbS nanoparticles,” *Sol. Energy Mater. Sol. Cells* **91**(5), 420–423 (2007). 666
- Q26

- 699 76. T. Jiu, P. Reiss, S. Guillerez, R. de Bettignies, S. Bailly, and F. Chandezon, "Hybrid solar  
700 cells based on blends of CdSe nanorods and poly(3-alkylthiophene) nanofibers," *IEEE J*  
701 *Sel Top. Quantum Electron.* **16**(6), 1619–1626 (2010).
- 702 77. R. J. Ellingson, M. C. Beard, J. C. Johnson, P. Yu, O. I. Micic, A. J. Nozik, A. Shabaev,  
703 and A. L. Efros, "Highly efficient multiple exciton generation in colloidal PbSe and PbS  
704 quantum dots," *Nano Lett.* **5**(5), 865–871 (2005).
- 705 78. H. A. Lorentz, "Über die Beziehung zwischen der Fortpflanzungsgeschwindigkeit des  
706 Lichtes der Körperdichte," *Ann. Phys. Lpz.* **9**, 641–665 (1880). Q27
- 707 79. L. Lorenz, "Über die Refraktionsconstante," *Ann. der Phys.* **11**, 70–103 (1880).
- 708 80. M. Born and E. Wolf, Chapter 2 in *Principles of Optics*, 7th (expanded) ed., Cambridge  
709 University, Cambridge, England (1999).
- 710 81. P. Carpena, V. Gasparian, and M. Ortuño, "Number of bound states of a Krönig-Penney  
711 finite-periodic Superlattice," *Eur. Phys. J. B* **8**, 635–641 (1999).
- 712 82. C. Cohen-Tannoudji, B. Diu, and F. Laloë, *Mécanique quantique*, Hermann, Paris  
713 (1997).
- 714 83. H. Li, "Refractive index of interdiffused AlGaAs/GaAs quantum well," *J. Appl. Phys.*  
715 **82**(12), 6251–6258 (1997).
- 716 84. S. V. Gaponenko, *Optical Properties of Semiconductor Nanocrystals*, Cambridge  
717 University Press, Cambridge, England (1998).
- 718 85. E. Kretschmann and H. Raether, "Radiative decay of non-radiative surface plasmons  
719 excited by light," *Z. Naturforsch. A* **23**, 2135 (1968). Q28
- 720 86. G. Mie, "Beiträge zur optik trüber medien, Speziell Kolloidaler Metallösungen," *Ann.*  
721 *Phys.* **330**, 377–445 (1908).
- 722 87. J. A. Polo Jr. and A. Lakhtakia, "Surface electromagnetic waves: A review," *Laser Pho-*  
723 *tonics Rev.* **5**, 234–246 (2011).
- 724 88. U. Kreibig and M. Vollmer, *Optical Properties of Metal Clusters*, Springer-Verlag, Berlin  
725 (1995).
- 726 89. L. Novotny, "Optical antennas tuned to pitch," *Nature* **455**, 887 (2008). Q29
- 727 90. K. Kneipp, Y. Wang, H. Kneipp, L. T. Perelman, I. Itzkan, R. R. Dasari, and M. S. Feld,  
728 "Single Molecule Detection Using Surface-Enhanced Raman Scattering (SERS)," *Phys.*  
729 *Rev. Lett.* **78**(9), 1667–1670 (1997).
- 730 91. B.-S. Yeo, J. Stadler, T. Schmid, R. Zenobi, and W. Zhang, "Tip-enhanced Raman  
731 Spectroscopy—Its status, challenges and future directions," *Chem. Phys. Lett.* **472**, 1–13  
732 (2009).
- 733 92. W. L. Barnes, A. Dereux, and T. W. Ebbesen, "Surface plasmon subwavelength optics,"  
734 *Nature (London)* **424**, 824–830 (2003).
- 735 93. B. Liedberg, C. Nylander, and I. Lundström, "Surface plasmon resonance for gas detection  
736 and biosensing," *Sens. Actuators* **4**, 299–304 (1983).
- 737 94. M.-K. Kwon, J.-Y. Kim, B.-H. Kim, I.-K. Park, C.-Y. Cho, C.-C. Byeon, and S.-J.  
738 Park, "Surface-plasmon-enhanced light-emitting diodes," *Adv. Mater.* **20**, 1253–1257  
739 (2008).
- 740 95. O. Stenzel, A. Stendhal, K. Voigtsberger, and C. Von Borczyskowski, "Enhance-  
741 ment of the photovoltaic conversion efficiency of copper phthalocyanine thin film de-  
742 vices by incorporation of metal clusters," *Sol. Energy Mater. Sol. Cells* **37**, 337–348  
743 (1995).
- 744 96. D. Derkacs, S. H. Lim, P. Matheu, W. Mar, and E. T. Yu, "Improved performance of  
745 amorphous silicon solar cells via scattering from surface plasmon polaritons in nearby  
746 metallic nanoparticles," *Appl. Phys. Lett.* **89**, 093103 (2006).
- 747 97. S. Pillai, K. R. Catchpole, T. Trupke, and M. A. Green, "Surface plasmon enhanced silicon  
748 solar cells," *J. Appl. Phys.* **101**, 093105 (2007).
- 749 98. R. B. Konda, R. Mundle, H. Mustafa, O. Bamiduro, A. K. Pradhan, U. N. Roy, Y. Cui, and  
750 A. Burger, "Surface plasmon excitation via Au nanoparticles in n-CdSe/p-Si heterojunction  
751 diodes," *Appl. Phys. Lett.* **91**, 191111 (2007).

99. J. Kim, K. Lee, N. Coates, D. Moses, T. Nguyen, M. Dante, and A. Heeger, “Efficient tandem polymer solar cells fabricated by all-solution processing,.” *Science* **317**, 222–225 (2007).  
Q30
100. D. Duche, P. Torchio, L. Escoubas, F. Monestier, J. J. Simon, F. Flory, and G. Mathian, “Improving light absorption in organic solar cells by plasmonic contribution,.” *Sol. Energy Mater. Sol. Cells* **93**, 1377–1382 (2009).  
754
101. S. Vedraïne, P. Torchio, D. Duché, F. Flory, J.-J. Simon, J. Le-Rouzo, and L. Escoubas, “Intrinsic absorption of plasmonic structures for organic solar cells,.” in *Sol. Energy Mater. Sol. Cells* **95**, S57–S64 (2011).  
Q31



**Francois Flory** graduated from Ecole Centrale Marseille in 1975, then received a PhD in optics in 1978 and a “Thèse d’Etat” in 1987. He is currently a professor “classe exceptionnelle” at Ecole Centrale Marseille. He was deputy director of this institution for 6 years and co-founded the optical cluster POPsud. He performs his research at the Institute for Materials, Microelectronics and Nanosciences, Marseille, France. His research interests are optical coatings and optical properties of nanostructured materials for different application fields such as solar cells, sensors, and light detectors. He is editor and co-author of the book *Thin Films for Optical Systems* (Marcel Dekker, 1995) and author of more than 200 publications, book chapters, patents, and conferences. He was the chairman of the conference Education and Training in Optics and Photonics (2005). He has been member of scientific committees of several international conferences and is a reviewer for several international scientific journals.



**Ludovic Escoubas** graduated from Centrale Marseille and received a PhD in optics in 1997. He is now a professor at Paul Cezanne University, Marseille, France and leader of the Optoelectronics Components and Photovoltaics (OPTO-PV) Team of IM2NP (CNRS Laboratory). His current research interests are micro- and nano-optical components and solar cells. He has authored more than 150 papers and communications, and he holds 6 patents.



**Gérard Berginc** received a Dipl. Engineer-Physicist degree from Ecole Centrale de Marseille and his doctorate in theoretical physics. He is currently a chief scientist and head of Advanced Research and Technology at Thales Optronique S.A. His research activities include high-frequency asymptotics, random volume and rough surface scattering, coherent effects in random media, and localization phenomena. He has authored or co-authored over 150 publications in books, journals and conferences, and is a Fellow Member of the Electromagnetics Academy. He holds more than 60 patents and was listed in *Who’s Who in Electromagnetism* and *Who’s*

*Who in the World.*

794 **Queries**

- 795 Q1: AU: Figure 2 is not sequentially cited after Fig. 1. Please cite Fig. 2.  
796 Q2: AU: Acronym RIE deleted because it was not used a second time throughout your paper.  
797 Q3: AU: Please verify edit to sentence beginning «The association» to ensure your meaning has  
798 been retained.  
799 Q4: AU: Please check use of double parens.  
800 Q5: AU: Please check correction of spelling (correct word ?).  
801 Q6: AU: Please provide definition of acronym SPPS.  
802 Q7: AU: Acronyms SERS, SEF, and SEIRA deleted because they were not used a second time  
803 throughout your paper.  
804 Q8: AU: Acronym TERS deleted because it was not used a second time throughout your paper.  
805 Q9: AU: Please provide definition of acronym BRDF and note that it may be deleted because it  
806 was not used a second time throughout your paper.  
807 Q10: AU: Please check grammar of sentence.  
808 Q11: AU: Please check: two page series in Ref. 1 ?  
809 Q12: AU: Please verify publisher and location in Ref. 6.  
810 Q13: AU: Please provide specific Phys. Rev. journal in Ref. 10 (for the year 1980).  
811 Q14: AU: Please check Refs. 13, 17, 43, and 44 for content errors, or provide the DOI.  
812 Q15: AU: Please check journal in Ref. 18.  
813 Q16: AU: Please update Ref. 25.  
814 Q17: AU: Please provide complete page series in Ref. 28.  
815 Q18: AU: Please check journal in Ref. 41 (as listed in AIP database).  
816 Q19: AU: Please provide complete page series in Ref. 47.  
817 Q20: AU: Please check publisher in Refs. 48 and 49 (spell out ?).  
818 Q21: AU: Please check page series in Ref. 56.  
819 Q22: AU: Please provide complete journal title for volume 568 and complete page series in Ref.  
820 58.  
821 Q23: AU: Please check page series in Ref. 60.  
822 Q24: AU: Please check publisher in Ref. 62 (spell out ?).  
823 Q25: AU: Please provide complete page series in Ref. 65.  
824 Q26: Disregard  
825 Q27: AU: Please check journal in Ref. 78 (not in AIP database).  
826 Q28: AU: Please check page series in Ref. 85.  
827 Q29: AU: Please check page series in Ref. 89.  
828 Q30: AU: Please provide complete page series in Ref. 99.  
829 Q31: AU: Please update Ref. 101.